national accelerator laboratory

NAL-29
2050

STUDY OF THE $\pi\pi$ SYSTEM FROM THRESHOLD TO 1 GEV

Ernest Malamud and Peter Schlein

May 1969

Operated by Universities Research Association Inc. Under Contract with the United States Atomic Energy Commission

NAL-29
2050

STUDY OF THE $\pi\pi$ SYSTEM FROM THRESHOLD TO 1 GEV*

Ernest Malamud
National Accelerator Laboratory

and

Peter Schlein
University of California, Los Angeles

Talk presented at Conference on the $\pi\pi$ and $K\pi$ Interactions
Argonne National Laboratory

May 1969

ABSTRACT

A detailed angular correlation analysis has been performed on a high statistics compilation of the reaction $\pi^- p \rightarrow \pi^- \pi^+ n$. This analysis, using the peripheral one-pion exchange dominated events, provided measurements of the following: (1) s-wave $\pi\pi$ phase shifts from the K-mass to 1 GeV, (2) ρ^0 parameters, and (3) certain combinations of the helicity amplitudes. The problem of using $\pi^- p \rightarrow \pi^- \pi^0 p$ to measure δ_S^2 is discussed. The phase shifts are compared with results from pole extrapolation and it is shown how the helicity amplitudes obtained can be used to make predictions for other reactions.

NAL-29
2050

STUDY OF THE $\pi\pi$ SYSTEM FROM THRESHOLD TO 1 GEV

Ernest Malamud
National Accelerator Laboratory

and

Peter Schlein
University of California, Los Angeles

Talk presented at Conference on the $\pi\pi$ and $K\pi$ Interactions
Argonne National Laboratory

May 1969

I. INTRODUCTION

There is a particular simplicity in spin 0-spin 0 elastic scattering analysis in the region where inelastic effects may be ignored, such that the determination of elastic phase shifts from on-mass-shell scattering data is considerably, with few assumptions, overdetermined. It was shown[1] that this simplicity carries over to the case in which an initial π scatters on a virtual π such that the initial state is not completely known because of absorption-like effects.

These constraints permit tests to be made of the overall consistancy of the OPE character of the interaction. In addition, the helicity amplitudes may be determined and are thus available to compare with the predictions of various theoretical models and also to predict observed cross sections for the related processes:

$$\pi^- p \rightarrow \pi^- \pi^+ n \tag{1a}$$

$$\pi^- p \rightarrow \pi^o \pi^o n \tag{1b}$$

$$\pi^+ p \rightarrow \pi^+ \pi^+ n. \tag{1c}$$

In an analysis[2] of reaction (1a) on a large sample of data in the range $0.6 \leq m_{\pi\pi} \leq 0.9$ GeV compiled from several laboratories we obtained the following results:

1. The data well satisfied the constraints of the model.

2. Values for the ρ^o parameters were obtained which are believed to be quite reliable within the context of one-pion exchange but which, however, disagree with the ρ^o width determined from e^+e^- colliding beam experiments.[3]

3. The T = 0 s-wave phase shift reached 90° in the vicinity of ~ 730 MeV.

4. Values for certain combinations of the helicity amplitudes are experimentally determined. These amplitudes are modified from their simple plane wave 0^-0^- scattering values by absorption effects on the initial state pion and the final state $\pi\pi$ system.

Since the compilation sample used for the original analysis covered the beam momentum range $2.1 < P_{lab} < 3.2$ GeV/c, we ignored the spread in P_{lab} and performed the analysis on the data with $\cos\theta_{CM} > 0.9$. This sample was divided into three $\cos\theta_{CM}$ ranges and thus the helicity amplitudes were actually determined as a function of $\cos\theta_{CM}$.

Furthermore, we obtained the $T = 2$ s-wave phase shift from the reaction $\pi^- p \to \pi^- \pi^0 p$ data which was also included in the compilation.

We report here a reanalysis of the data with the following modifications in the procedure:

1. The data sample is divided into $m_{\pi\pi}$ and momentum transfer t bins. This procedure, described in detail below, is a more satisfactory way to handle a spread in beam momentum.

2. The helicity amplitudes are given an explicit t dependence Ae^{-bt}, shown to be valid for the range of t covered by the data (we use a metric where $t > 0$ in the physical region).

3. δ_s^2 is obtained from a pole extrapolation analysis of $\pi^- p \to \pi^- \pi^- \Delta^{++}$.

4. An experimental resolution function has been added to the analysis.

5. In addition to a fit in the ρ-region (600-900 MeV), fits were also performed down to the K-mass and the results shown to agree with pole extrapolation results.

The results for δ_s^0 are seen not to be sensitive to these changes in procedure, although a more useful parametrization of the empirical helicity amplitudes has resulted.

II. DATA COMPILATION

The data compilation used is summarized in Table I. The total of 68356 events in this πp compilation[1] cover 4 reactions and a large beam momentum range. Most of the groups who have contributed data to this compilation have representatives at this conference. I want to express our gratitude to these bubble-chamber groups who have allowed us to use their events in this analysis.

Table I. Data Compilation.[a]

Institution	P_{lab} GeV/c	Initial State	Numbers of Events $\pi^-\pi^+n$	$\pi^-\pi^o p$	$\pi^-\pi^-\pi^+p$	$\pi^-\pi^+\pi^+p$
U. of Pennsylvania	2.14, 3.0	π^-p	2234	1582		
Saclay, Orsay, Bari Bologna	2.75	π^-p	3365	2026		
Purdue Univ.	2.7	π^-p	4402	3014	2131	
Univ. of Rochester, Yale Univ.	6.94	π^+p				2013
LRL Berkeley (Chung)	3.2, 4.2	π^-p			10117	
LRL Berkeley (Gidal)	3.0 - 4.0	π^+p				7308
LRL Berkeley (Jacobs)	2.05 - 3.22	π^-p	7787	6032		
LRL Berkeley (Goldhaber)	3.65	π^+p				1787
U.C. San Diego	3.2, 3.5	π^+p				3663
Brookhaven	6.0	π^-p			675	
Argonne, U. of Toronto, Wisconsin	3.0	π^-p	2767	1882	1715	
Columbia - Rutgers	8.4	π^+p				3856
Total = 68356 Events			20555	14536	14638	18627

[a]See Ref. 1.

III. MODEL FOR MOMENT ANALYSIS

It was suggested[1] that both the $\pi\pi$ phase shifts and the helicity amplitudes for reaction (1) may be extracted from the data in highly overconstrained fits, using only a small subset of the assumptions of the absorption model, all of which have observable consequences and which may therefore be subjected to test.

The fundamental assumption common to one-pion-exchange with and without absorption is that the amplitude to reach the final state in reaction (1) with given $\pi\pi$ relative orbital angular momentum ℓ, can be factored into two parts, one of which is the amplitude for ℓ-wave $\pi\pi$ scattering $A^{\ell}_{\pi\pi} \sim e^{i\delta_\ell} \sin \delta_\ell$. Thus we write $A^{\ell}_{\pi\pi} \times M^{\lambda\lambda'}_{\ell\mu}$ as the amplitude to reach a final state containing a $\pi\pi$ system with internal angular momentum ℓ and helicity μ and a nucleon with helicity λ from an initial state with nucleon helicity λ'. The helicity amplitudes $M^{\lambda\lambda'}_{\ell\mu}$ are functions of the total CM energy, E^*, momentum transfer to the neutron, t, and the effective mass of the $\pi\pi$ system, $m_{\pi\pi}$. In addition to the basic factorization assumption we assume:

1. The helicity amplitudes are relatively real.

2. The $\pi\pi$ scattering is elastic up to 1 GeV, the highest mass studied.

3. Only s- and p-waves are necessary to explain the observed distributions.

4. Production from an unpolarized target is assumed and a sum is made over the final state nucleon helicity variable.

The argument of the spherical harmonic moments is the unit vector of the outgoing π^- in the $\pi^-\pi^+$ rest frame: the coordinate system is chosen in this rest frame such that the $\tilde{y}$ axis lies along the normal to the production plane $\hat{n} \sim \hat{P}_{in} \times \hat{P}_{out}$, and the $\tilde{z}$ (polar) axis is defined to be the direction of motion of the $\pi\pi$ system. Thus the consequence of parity conservation on the helicity amplitudes (valid for any ℓ) is the relation

$$M_{\ell,-\mu}^{-\lambda,-\lambda'} = (-1)^{\mu+\lambda+\lambda'} M_{\ell,\mu}^{\lambda,\lambda'}, \tag{2}$$

and the $\langle \mathrm{Im}\, Y_\ell^m \rangle$ moments vanish. This reduces the number of independent helicity amplitudes for each ℓ from $4(2\ell+1)$ to $2(2\ell+1)$. Thus for s- and p-wave $\pi\pi$ scattering there are 8 independent amplitudes.

It is convenient to express these helicity amplitudes as components of 2-component vectors:

$$\vec{s} = (M_{0,0}^{++}, M_{0,0}^{-+}) \tag{3a}$$

$$\vec{p}_1 = (M_{1,1}^{++}, M_{1,1}^{-+}) \tag{3b}$$

$$\vec{p}_0 = (M_{1,0}^{++}, M_{1,0}^{-+}) \tag{3c}$$

$$\vec{p}_{-1} = (M_{1,-1}^{++}, M_{1,-1}^{-+}), \tag{3d}$$

where the superscripts (++, -+) refer to nucleon non-flip and flip, respectively. The observable experimental quantities can be expressed[1]

in terms of the $A^{\ell}_{\pi\pi}$ and $\vec{s}$, $\vec{p}_i$ vectors as:

$$\frac{d^2\sigma}{dmdt} = |A^P_{\pi\pi}|^2 \left\{ |\vec{p}_1|^2 + |\vec{p}_o|^2 + |\vec{p}_{-1}|^2 \right\} + |A^S_{\pi\pi}|^2 \left\{ |\vec{s}|^2 \right\} \tag{4a}$$

$$\frac{d^2\sigma}{dmdt} \langle Y^o_1 \rangle = \frac{2}{\sqrt{4\pi}} \operatorname{Re}\left(A^S_{\pi\pi} A^{P*}_{\pi\pi}\right) \left\{ \vec{p}_o \cdot \vec{s} \right\} \tag{4b}$$

$$\frac{d^2\sigma}{dmdt} \langle \operatorname{Re} Y^1_1 \rangle = \frac{1}{\sqrt{4\pi}} \operatorname{Re}\left(A^S_{\pi\pi} A^{P*}_{\pi\pi}\right) \left\{ \vec{s} \cdot \left(\vec{p}_1 - \vec{p}_{-1}\right) \right\} \tag{4c}$$

$$\frac{d^2\sigma}{dmdt} \langle Y^o_2 \rangle = \frac{2}{\sqrt{20\pi}} |A^P_{\pi\pi}|^2 \left\{ |\vec{p}_o|^2 - \frac{1}{2} \left(|\vec{p}_1|^2 + |\vec{p}_{-1}|^2 \right) \right\} \tag{4d}$$

$$\frac{d^2\sigma}{dmdt} \langle \operatorname{Re} Y^1_2 \rangle = \sqrt{\frac{3}{20\pi}} |A^P_{\pi\pi}|^2 \left\{ \vec{p}_o \cdot \left(\vec{p}_1 - \vec{p}_{-1}\right) \right\} \tag{4e}$$

$$\frac{d^2\sigma}{dmdt} \langle \operatorname{Re} Y^2_2 \rangle = \sqrt{\frac{6}{20\pi}} |A^P_{\pi\pi}|^2 \left\{ -\vec{p}_1 \cdot \vec{p}_{-1} \right\} \tag{4f}$$

such that

$$\frac{d^4\sigma}{dmdtd\Omega_{\pi\pi}} = \frac{d^2\sigma}{dmdt} \left\{ \sum_{\ell=0}^{2} \sum_{m=-\ell}^{+\ell} \langle Y^m_\ell \rangle \; Y^m_\ell \right\} .$$

The convenience of these vectors lies in the fact that all the helicity amplitude quantities in Eqs. (4) are just dot products of $\vec{s}$, $\vec{p}_1$, $\vec{p}_o$, and $\vec{p}_{-1}$. It may be seen that seven combinations of the $\vec{s}$, $\vec{p}_i$ vectors occur in Eqs. (4). These seven combinations are completely determined by the following 6 quantities which we use as variables in the fits described below:

$$|\vec{s}|,\ |\vec{p}_o|,\ |\vec{p}_1-\vec{p}_{-1}|,\ \theta_{s,p_o},\ \theta_{s,p_1-p_{-1}},\ \left(|\vec{p}_1|^2+|\vec{p}_{-1}|^2\right)^{\frac{1}{2}},$$

where $\theta_{s,p_o}\left(\theta_{s,p_1-p_{-1}}\right)$ is the angle between $\vec{s}$ and $\vec{p}_o$ ($\vec{s}$ and $\vec{p}_1-\vec{p}_{-1}$). One constraint thus exists between the first five quantities; the last quantity requires the vectors $\vec{p}_1$ and $\vec{p}_{-1}$ to originate at an arbitrary point on a circle whose center is at the midpoint of the vector $\vec{p}_1-\vec{p}_{-1}$. The radius of this circle is given by:

$$\text{Radius} = \frac{1}{2}\sqrt{2\left(|\vec{p}_1|^2+|\vec{p}_{-1}|^2\right)-|\vec{p}_1-\vec{p}_{-1}|^2}\ , \tag{5}$$

as shown in the figure:

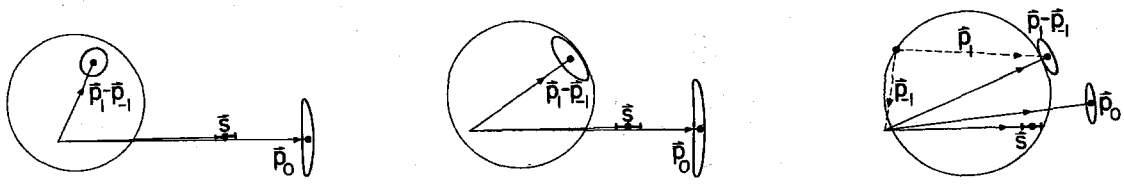

Note that Eqs. (4) are invariant under rotations and reflections in the plane of the vectors and no generality is lost if $\vec{s} = \left(|\vec{s}|,\ 0\right)$ is assumed. In addition, the equations are invariant under the transformation $\vec{p}_1 \leftrightarrow -\vec{p}_{-1}$. These invariances are due to the fact that no polarizations are measured in the type of experiment discussed here. Subject to these stated indeterminicies, the helicity amplitudes are obtained from the fit described below as a function of momentum transfer and may be compared with various theoretical predictions.

IV. PROBLEMS CONNECTED WITH THE DETERMINATION OF δ_s^2

In order to determine δ_s^o from an analysis of the $\pi^-\pi^+n$ reaction, it is necessary to input independent information on δ_s^2. We present the following discussion of the problems connected with the determination of δ_s^2.

δ_s^2 can be determined either by analyzing the s, p interference in the $\pi^-\pi^o p$ reaction or by extrapolating to the pion exchange pole in $\pi^-\pi^-\Delta^{++}$ or $\pi^+\pi^+n$. The s,p interference was studied in a pole extrapolation analysis of $\pi^-\pi^o p$ by Baton, Laurens, and Reignier.[5] However, there is a particular difficulty in using $\pi^-\pi^o p$ to obtain δ_s^2 that casts some doubts on the validity of their result for $m_{\pi\pi} \lesssim m_\rho$. Consider the following reactions:

$$\pi^-p \rightarrow \pi^-\pi^+n \tag{6a}$$

$$\pi^+p \rightarrow \pi^-\pi^+\Delta^{++} \tag{6b}$$

$$\pi^-p \rightarrow \pi^-\pi^-\Delta^{++} \tag{6c}$$

$$\pi^+p \rightarrow \pi^+\pi^+n \tag{6d}$$

$$\pi^-p \rightarrow \pi^-\pi^o p. \tag{6e}$$

The first four of these reactions are produced with charge exchange to the nuclear system and therefore are well suited for studying the π-exchange process, whereas in the remaining final state, $\pi^-\pi^o p$, neutral exchange occurs and therefore ω-exchange can also contribute. There

is considerable evidence that in fact, ω-exchange does contribute to $(\pi^-\pi^o)p$ production and that it becomes more and more important as $m_{\pi\pi}$ decreases below m_ρ. There are the following three types of evidence for this.

1. Comparison between the shape of $d\sigma/dt$ for $(\pi^-\pi^o)p$ and $(\pi^-\pi^+)n$.

2. Comparison between the magnitude of $d\sigma/dt$ for $(\pi^-\pi^o)p$ for $m_{\pi\pi} \sim m_K$ and the magnitude expected from reactions (6c) and (6d).

3. Evidence for increasing contribution to non-zero helicity p-wave states below the ρ-peak in $\pi^-\pi^o p$.

Let us examine these in turn. Figure 1(a) compares dN/dt for $\pi^-\pi^+n$ and $\pi^-\pi^o p$ in the ρ-region (600-900 MeV). The solid curve drawn on the $\pi^-\pi^o p$ plot is one half the dN/dt distribution for $\pi^-\pi^+n$, which is what is expected for $\pi^-\pi^o p$ if only p-wave π-exchange contributes. We see dN-dt is both flatter and larger for $\pi^-\pi^o p$.

Figure 1(b) shows the $\pi\pi$ scattering angular distribution for 5837 $\pi^-\pi^+n$ and 3199 $\pi^-\pi^o p$ events in the ρ-region (600 to 900 MeV) with $\cos\theta_{CM} > 0.9$. The curves shown are calculated from the $\langle Y_1^o \rangle$ and $\langle Y_2^o \rangle$ moments in the data. For both reactions s- and p-wave are sufficient to describe the distributions. The insert shows the values of the m = 0 moments. (See comments in Ref. 2 on apparent negative moments for $\ell > 2$.)

In Fig. 2, $d\sigma/dt$ distributions of reactions (6a), (6b), (6c), and (6e) are plotted for $460 < m_{\pi\pi} < 540$ MeV. Only the highest statistics $\pi^-\pi^-\Delta^{++}$ and $\pi^-\pi^+\Delta^{++}$ momenta are used. For $\pi^-\pi^+n$, all beam momenta

are combined (2.1 - 3.2 GeV/c). For $\pi^-\pi^o p$ the same thing is done except a minimum t of 0.06 GeV^2 is imposed to avoid the region biased by missing short proton recoils. The curves superimposed on the data are calculated from the appropriate OPE equation modified by the Dürr-Pilkuhn vertex correction factors[6] and with the appropriate s-wave $\pi\pi$ cross section chosen to normalize the curves to the data in the $\pi^+\pi^-$ and $\pi^-\pi^-$ cases. A consistent $\sigma_s^{\pi^-\pi^+} \simeq 22\text{-}26$ mb is found to agree with both $\pi^-\pi^+ n$ and $\pi^-\pi^+\Delta^{++}$ reactions. As discussed below, the indicated value of $\sigma_s^{T=2} = 18$ mb obtained this way is about a factor of two too large due to background in $\pi^-\pi^-\Delta^{++}$. Nevertheless it may be noted that even with this correction to the prediction for $\pi^-\pi^o p$, the experimental $d\sigma/dt$ for $\pi^-\pi^o p$ is in complete disagreement with the other π-exchange process, presumably due to the presence of ω exchange.

Finally, we show in Fig. 3(b) the $\langle Y_2^m \rangle$ moment quantities[2] multiplied by the mass spectrum for the $\pi^-\pi^o$ system in $\pi^-\pi^o p$. The $\langle Y_2^m \rangle$ moments for $\pi^-\pi^o p$ do not all have the same dependence on $m_{\pi\pi}$, in constrast[2] with the situation for $\pi^-\pi^+ n$ shown in Fig. 3(a). Furthermore $\langle \mathrm{Re}Y_2^2 \rangle \neq 0$ for $\pi^-\pi^o p$, again in contrast with $\pi^-\pi^+ n$. An increasing contribution of non-zero helicity p-wave $\pi^-\pi^o$ production with decreasing $m_{\pi\pi}$ would have just such an effect.

The above arguments point to the fact that there is an increasing contribution of ω exchange to the p-wave $\pi^-\pi^o$ production below the ρ-mass. Since the T = 2 s-wave $\pi\pi$ system cannot be fed by ω exchange, we have the unusual situation that the s-wave $\pi^-\pi^o$ system results from

π-exchange and that the p-wave $\pi^-\pi^0$ system results dominantly from ω-exchange. In effect, therefore, the s- and p-wave Argand diagrams are rotated relative to one another by an unknown angle which is the phase difference of the π- and ω-exchange components. It is clear that in an analysis of $\pi^-\pi^0 p$, without knowing the phases of the π- and ω-exchange components, the sp interference measurements cannot be used to determine the relative s,p phase shift in the scattering.

It seems that the only reliable way to obtain δ_s^2 at present is to perform a pole extrapolation analysis of $\pi^-\pi^-\Delta^{++}$ or $\pi^+\pi^+n$. Following the procedure suggested by Ma et al.[7] in their analysis of $pp \to \Delta^{++}n$ and discussed yesterday,[8] in which Dürr-Pilkuhn[6] modified OPE is used as a normalizing function in the pole extrapolation, Colton et al.[9] have extrapolated the following quantity to the pion exchange pole for $\pi^-\pi^-\Delta^{++}$ and $\pi^-\pi^+\Delta^{++}$:

$$"\sigma" = \frac{(d\sigma/dt)_{exp}}{(d\sigma/dt)_{DP-OPE}} , \tag{7}$$

using the fit "σ" = a + bt. The bt term allows for a linear departure of $(d\sigma/dt)_{DP-OPE}$ from $(d\sigma/dt)_{exp}$ which, since DP-OPE is already such a good description of the experimental t-distribution, is quite sufficient at the present level of statistics. Colton et al. find that $\sigma_s^{T=2} \sim 9.5$ mb throughout the ρ-region. This corresponds to $\delta_s^2 = -21°$ at 770 MeV. These results agree with the preliminary data of Gidal et al.[10] in studying $\pi^+p \to \pi^+\pi^+n$ at 2.75 GeV/c.

Thus in the moment analysis of $\pi^- \pi^+ n$ described below, we have used values of δ_s^2 which correspond to $\sigma_s^{T=2} = 9.5$ mb throughout the mass region considered. We think this is the most reliable value available.

V. RESULTS OF THE MOMENT ANALYSIS

The analysis was performed on a 7319 event low-momentum transfer subsample of reaction (1). The events were binned in the Chew-Low plane as shown in Fig. 4. The $m_{\pi\pi}$ bins are 20 MeV wide between 600 and 1000 MeV and 40 MeV wide below. Each of the 25 $m_{\pi\pi}$ bins is then divided into several t-bins using the criterion that there be a sufficient number of events in each bin to give reliable errors on the moments. The Chew-Low boundaries are drawn for the upper and lower center-of-mass energy limits of the data and for a representative median energy.

It was found that a given spherical harmonic moment was a function of t and m only and not of the beam momentum, P_{lab}, over the range available. This would be the case if all the helicity amplitude quantities in Eqs. (4) had the same dependence on P_{lab}. Thus for each of the bins in Fig. 4, the quantities $d^2\sigma/dtdm$, $\langle Y_1^0 \rangle$, $\langle \mathrm{Re} Y_1^1 \rangle$, $\langle Y_2^0 \rangle$, $\langle \mathrm{Re} Y_2^1 \rangle$, $\langle \mathrm{Re} Y_2^2 \rangle$ were evaluated.

It was suggested in Ref. 1 that in the ρ region where the $\pi\pi$ phase shifts are rapidly varying, the $m_{\pi\pi}$ dependence of the helicity amplitudes could be ignored. Bander, Shaw, and Fulco[11] later showed of the basis of the absorption model that this assumption was valid over the mass region

used in Ref. 2, namely 600-900 MeV but suggested that at lower mass one could expect somewhat different $m_{\pi\pi}$ dependencies for the various helicity amplitudes. Thus we regard the 600-900 MeV fit as the most reliable, although later when discussing the phase shift situation at the K-mass, we present fits for 400 or 480 MeV to 1000 MeV. In any case, there are no significant differences between these fits and acceptable χ^2's result for all of them.

For the 600-900 MeV fit, there are a total of 88 (m, t) bins and thus $6 \times 88 = 528$ data points. The following 30 quantities were variables in the fit, making it a 498 constraint fit:

1. δ_s^o at 15 $m_{\pi\pi}$ values (every 20 MeV for 600-900 MeV).
2. The ρ-parameters m_ρ and Γ_ρ.

The p-wave given by a Breit-Wigner amplitude:

$$\cot \delta_\rho = \frac{(m_\rho^2 - m_{\pi\pi}^2)\left[1 + \left(\frac{q}{q_\rho}\right)^2\right]}{2m_\rho \Gamma_\rho \left(\frac{q}{q_\rho}\right)^3}, \tag{8}$$

where q_ρ and q are the $\pi\pi$ cm decay momenta for $\pi\pi$ systems of mass m_ρ and $m_{\pi\pi}$, respectively, and m_ρ and Γ_ρ are variables in the fit.

3. 11 helicity amplitude quantities. As mentioned in an earlier section the six helicity amplitude quantities shown below in Eqs. (9) were assumed to have an exponential dependence on t, Ae^{-bt}, over the range of data. We demonstrate below that this is a good assumption. Since there is an

overall normalization which is determined by the experimental cross section at the mean beam momentum, in the fit we arbitrarily use $A = 1$ in Ae^{-bt} for the first helicity amplitude quantity. Thus the 11 variables are

$$|\vec{s}| = e^{-b_1 t} \tag{9a}$$

$$|\vec{p}_o| = A_2 e^{-b_2 t} \tag{9b}$$

$$\theta_{s,\, p_o} = A_3 e^{-b_3 t} \tag{9c}$$

$$|\vec{p}_1 - \vec{p}_{-1}| = A_4 e^{-b_4 t} \tag{9d}$$

$$\theta_{s,\, p_1 - p_{-1}} = A_5 e^{-b_5 t} \tag{9e}$$

$$\sqrt{|\vec{p}_1|^2 + |\vec{p}_{-1}|^2} = A_6 e^{-b_6 t} \tag{9f}$$

4. In addition we allowed two degrees of freedom for the mass dependence of the helicity amplitude quantities by assuming that each of the above exponentials was multiplied by the factor

$$g(m_{\pi\pi}) = 1 + a(m_{\pi\pi} - 0.75) + b(m_{\pi\pi} - 0.75)^2.$$

Since the fit is to the six $d^2\sigma/dtdm$ and $\langle Y_\ell^m \rangle$ quantities, and the $\langle Y_\ell^m \rangle$ depend on the ratio of helicity amplitudes, any common factor in the helicity amplitudes cancels out and the $g(m_{\pi\pi})$ factor only enters into the

$d^2\sigma/dtdm$ terms in the χ^2. We also fold a resolution function with σ = 14 MeV into the calculated distribution function before computing the χ^2 in the fit.

Since the different contributions to the Chew-Low plot in Fig. 4 do not all contribute to the bins near the Chew-Low boundaries, it was necessary to correct for this. In addition, the different beam momentum contributions each have different track lengths as well as the factorizable P_{lab}^{-2} dependence. All three of these factors are taken into account by means of the following procedure. In forming the χ^2, the calculated value of $d^2\sigma/dtdm$ (with arbitrary normalization) for each (m,t) bin is multiplied by a weighting factor

$$W = \sum_K \frac{(N_{meas})_K}{(N_{calc})_K} f_K, \tag{10}$$

where the summation, K, is over the P_{lab} contributions, $(N_{calc})_K$ is the calculated number of events integrated over the entire portion of the grid used for the fit lying inside the physical region for the Kth P_{lab} value, $(N_{meas})_K$ is the experimentally observed number of events at that P_{lab} in the grid used for the fit, and f_K is the fraction of the bin ($0 \leq f_K \leq 1.0$) lying inside the physical region for that P_{lab}.

Tables II-IV give values of the parameters resulting from the fits. A_1, A_2, A_4, and A_6 are in units of $(\mu b/MeV\ GeV^2)^{\frac{1}{2}}$. These factors include the μbarn equivalent of the data of 5.3 ev/μb which could be uncertain

by ~ 10% due to systematic errors in the cross section used. A cross section of 3.8 mb is assumed.

Fits to the 600-900 data using in turn the Baton et al.[5] δ_s^2 values and those of Colton et al.[9] are given in Tables II-IV for the three solutions reported earlier: DOWN-UP, UP-UP, and UP-DOWN. The α columns contain the results when the Baton et al. δ_s^2 were used and the γ columns contain the results using the Colton et al. δ_s^2. The results on δ_s^o and the helicity amplitude quantities are seen not to be very sensitive to this change in δ_s^2. The results shown in columns γ and δ also include a 14 MeV wide resolution folded into the calculated distribution function before computing the χ^2 in the fit. The δ_s^o's from the γ fit are plotted in Fig. 5.

The resulting confidence levels are quite good, ranging from 13%-50% for the various cases for this 498 constraint fit. We may conclude that the model is indeed compatible with the data over this range of $\pi\pi$ mass. There are no significant differences in δ_s^o from our earlier fit obtained using $\cos\theta_{CM}$ selection[2] although there seems to be a slight upward shift in both m_ρ and Γ_ρ from the earlier values of 767 and 149 MeV, respectively, apparently resulting from the fact that a $\cos\theta_{CM}$ cut introduces a kinematic narrowing of the resonance peak.

Despite the warning of Bander, Shaw, and Fulco,[11] we have also performed fits to the data over the entire 400-1000 MeV mass range. There are now 118 × 6 data points and 40 free parameters; thus, they are 668 constraint fits. These are shown for each of the solutions in

the β columns of Tables II-IV. Column β uses Baton et al.[5] δ_s^2 and column δ uses Colton et al.[9] δ_s^2. The significant result in this case is the substantial decrease in confidence levels (1-4%) indicating that some aspect of the model is being strained. Still, these confidence levels are not unacceptable and one may compare the results with the 600-900 MeV fits. The δ_s^o values are plotted in Fig. 6. There again does not seem to be any substantial change in the results.

VI. PREDICTIONS FROM FITS

The data have been fit assuming a simple model in which the $m_{\pi\pi}$ and t dependencies have been factored out. The P_{lab}^{-2} factor of OPE was not used but can now be assumed and predictions made of $d\sigma/dt$ for $\pi^- p \rightarrow \pi^- \pi^+ n$ at different P_{lab} values. The fitted model calculation was normalized to the experimental cross section at P_{lab} = 2.7 GeV/c, the mean P_{lab} of the compiled $\pi^+ \pi^- n$ data. Assuming the P_{lab}^{-2} factor of OPE, and using the δ_s^o values, the ρ-parameters and the helicity amplitudes with their t-dependencies from column α of Table III, the curves shown in Fig. 7 were obtained. For purposes of that figure, the compilation data were divided into three P_{lab} bins and the experimental $\pi^- \pi^+ n$ cross sections and μbarn equivalent numbers for each sample of data used to plot the data.

We can go outside the range of the compilation and make predictions. The agreement is quite good at higher laboratory momenta, 4.0[12] and 8.0[13] GeV/c and fairly good at lower momentum, 1.59 GeV/c[14] with some slight indication here that this parameterization is beginning to fail.

Since the $d\sigma/dt$ predictions are successful in the ρ-region, we now examine $d\sigma/dt$ predictions at the K-mass in Fig. 8. The low t peaking still seems to be present although of course the statistics are poorer now. The calculated curves are derived from the parameters in column β in Table III and are seen to agree fairly well with the data. It should be noted that these curves cannot be used to resolve the phase shift ambiguity since the product of the helicity amplitude factor and $\sin^2 \delta_s^o$ is about the same for all three solutions; i.e., if δ_s^o is decreased, there is a compensating increase in the helicity amplitude.

To make predictions for reactions (1) or their neutron target equivalents using the values of the parameters in Tables II-IV, the parameters in Eqs. (4) must be multiplied by $1.0/P_{lab}^2$. A_1 is not a parameter in the fit but is obtained from the overall normalization.

As an example of how to use Tables II-IV to make predictions, suppose one wants to describe $\pi^- p \to \pi^o \pi^o n$ at 2.37 GeV/c using the UP-UP fit (Table III) in column γ.

$$\frac{d^2\sigma}{dm_{\pi^o\pi^o}(\mathrm{MeV})dt}\,(\mu b/\mathrm{MeV\ GeV}^2) = \frac{g(m_{\pi\pi})}{P_{lab}^2}\left\{\left(A_1 e^{-b_1 t}\right)^2 |A_s|^2\right\} \tag{11}$$

$$\frac{d^2\sigma}{dm_{\pi^o\pi^o}(\mathrm{MeV})dt} = \frac{1+0.48\left[m_{\pi\pi}(\mathrm{GeV})-0.75\right]+3.0\left[m_{\pi\pi}(\mathrm{GeV})-0.75\right]^2}{(2.37)^2} \times$$
$$\times \left\{\left[16.4\, e^{-7.48t\,(\mathrm{GeV})}\right]^2 |A_s|^2\right\}, \tag{12}$$

where

$$|A_s|^2 = \frac{2}{9}\sin^2\delta_s^o + \frac{2}{9}\sin^2\delta_s^2 - \frac{4}{9}\sin\delta_s^o\sin\delta_s^2\cos\left(\delta_s^2 - \delta_s^o\right). \quad (13)$$

This can then be integrated over any part of the physical region of the Chew-Low plot to produce $m_{\pi^o\pi^o}$ or t projections.[23]

VII. EXTRAPOLATION TO THE POLE USING DÜRR-PILKUHN DESCRIPTION OF THE CHEW-LOW INTENSITY DISTRIBUTION

The question naturally arises as to whether the phase shifts determined in the analysis described above are appreciably altered by the fact that one of the pions in the collision is virtual. It is quite interesting to attempt a pole extrapolation of the intensity distribution. This has been done using the Dürr-Pilkuhn[6] modified OPE formula on 6051 $\pi^-\pi^+n$ events bounded by $0.6 < m_{\pi\pi} < 0.9$ GeV and $0 < t < 0.2$ GeV^2. Each event is characterized by 3 numbers: P_{lab}, $m_{\pi\pi}$, and t. The maximum likelihood procedure obviates the need for any special technique for handling the spread in laboratory momentum such as was needed for the fits using binned data. The disadvantage of the maximum likelihood method is the excessive amount of computer time required.

In the fits performed the constant c in the form factor, $(c - \mu^2/c + t)^2$ used by Wolf[15] is held constant at Wolf's value $c = 2.29$ GeV^2. The neutron "radius", R_n, is fixed at $R_n = 2.3$ GeV^{-1}.

There are only 3 free parameters: R_ρ and two s-wave "phase shifts,"[16] one at 600 MeV and one at 900 MeV with straight line interpolation in between them; optimization is made to the shape of the distribution.

The fits are very insensitive to the s-wave since only the intensity distribution in the Chew-Low plane is used. The s-wave can only be determined at all insomuch as the mass spectrum deviates from a Breit-Wigner and the t-dependencies of s- and p-waves are different.

The s-wave amplitude from the 600 MeV - 900 MeV (best) run is given by

$$A_s = \sin\left[(1.13 \pm 0.21) + \left(\frac{m_{\pi\pi} - 0.6}{0.9 - 0.6}\right)(2.26 \pm 0.29)\right] . \qquad (14)$$

Thus although this straight line is started out more steeply than the "DOWN-UP" branch it converges to a slope approximating the "UP-UP" solution.

The value for $R\rho$ from the (best) run is (4.0 ± 1.4) GeV^{-1} to be compared with Wolf's[15] value of 8.28.

A series of runs are made with various values for m_ρ and Γ_ρ. The results are likelihood contours in the m_ρ, Γ_ρ plane. A least squares quadratic fit to these values yields best values and 1 S.D. errors:

$$m_\rho = 768.4 \pm 2.4$$
$$\Gamma_\rho = 148.1 \pm 4.7 \ ,$$

$d\sigma/dt$ predictions in the ρ-region, using parameters from the fits are shown as dotted curves on Fig. 7. The experimental cross section was not used in the maximum likelihood fit which was only to the shape of the distribution. However, the $d\sigma/dt$ predictions which are absolute agree remarkably well with the data.

VIII. PHASE SHIFTS AT THE K-MASS

Our best knowledge of the situation at the K-mass is summarized as follows:

From the pole-extrapolation analysis[9] of $\pi^-\pi^-\Delta^{++}$ 3.2 GeV/c

$$\delta_s^2 = -(12 \pm 3)^\circ .$$

From a moment analysis of $\pi^-\pi^+n$ using a T = 2 compatible with the above value and a resolution function on the mass the "UP-UP" solution gives $\delta_s^o = (41 \pm 5)^\circ$ (column γ in Table III).

Pole-extrapolation analysis[9] of both $\pi^-\pi^+n$ and $\pi^-\pi^+\Delta^{++}$ using the Dürr-Pilkuhn equations for normalization gives results compatible with the above.

Using these numbers $\delta_s^o - \delta_s^o = (53 \pm 6)^\circ$. This phase-shift difference is well within the T-violation area of the Casella diagram.[17] The corresponding angle for ϵ', the CP violating amplitude in K^o and $\bar{K}^o$ decay is $(37 \pm 6)^\circ$ which favors the first quadrant solution for η_{oo} assuming $|\epsilon'| \neq 0$.

An independent measurement of $|\delta_s^o - \delta_s^2|$ comes from the K_1^o decay branching ratio. Two measurements have been reported. Morfin and Sinclair,[18] in a paper appended to this one, obtain $(68 \pm 11)^\circ$ or $(74 \pm 10)^\circ$ depending on what is assumed for the electromagnetic correction. The published result of Gobbi et al.[19] is $\left(39^{+13}_{-18}\right)^\circ$.

There is a considerable amount of controversy, both theoretical and experimental, as to the phase shifts at the K-mass. We have already pointed out the unreliability of the small δ_s^2 value obtained in the $\pi^-\pi^o p$ reaction. Among the phase shifters the choice for δ_s^o is between the "DOWN" or "UP" branch. We shall return to this point later.

IX. PROBLEM OF THE RHO WIDTH

The maximum likelihood pole extrapolation analysis on the $\pi^-\pi^+ n$ data without a resolution function added indicates a shrinking of the width by about 13 MeV.

Although a compilation of data from several experiments is useful for many things, one thing it is not very good for is determining the resonance parameters of a broad resonance. Systematic errors in the mass calibration from one experiment to another may be present. This error was estimated by doing the moment fits separately on data from different laboratories and may contribute another 10 MeV to the width.

If a total 23 MeV of correction is applied to our latest result obtained with new values of the T = 2 phase shifts and a resolution function, the corrected value, $\Gamma_{\rho^o} = 132 \pm 13$ MeV, is obtained. It is clear from this however that the present compilation is incompatible with the very narrow widths around 100 MeV that have been reported.[3]

X. DISCUSSION OF PHASE SHIFT AMBIGUITIES

One of the major goals in this work is to try and arrive at an unique solution for δ_s^o. Above the ρ the "DOWN" branch seems to be ruled out by the drop-off in the $\pi^o\pi^o$ spectra,[20,21] but can really only be resolved by new high beam momentum $\pi^o\pi^o$ experiments.

An important test of the δ_s and the δ_p determinations is to see if the same results are obtained from an analysis of $\pi^+p \rightarrow \pi^-\pi^+\Delta^{++}$. The results described in a paper appended to this one[22] were obtained with a cos θ selection. The same three T = 0 s-wave $\pi\pi$ phase shift solutions found in the $\pi\pi n$ analysis are found again. The "UP-DOWN" solution (constant $\delta_s^o \sim 90°$) has an unacceptably low confidence level, thus strengthening the conclusion previously reached that "UP-DOWN" was unlikely from comparison with the $\pi^o\pi^o$ spectra. These results, aside from providing us with good evidence that we are actually measuring $\pi\pi$ phase shifts and not something characteristic of the $\pi\pi n$ or $\pi\pi\Delta$ reactions reinforce the conclusion previously reached that there exists a T = 0 scalar meson.

Below the ρ the situation is more complicated but the evidence favors the "UP" branch mainly based on comparison with Chew-Low extrapolation on both $\pi^-\pi^+n$ and $\pi^-\pi^+\Delta^{++}$.[9]

The "UP-UP" and "DOWN-UP" solutions show very different behavior for the $\vec{s}$, $\vec{p}$ vectors. In the "UP-UP" case $\vec{p}_o$ is parallel to $\vec{s}$, whereas in the "DOWN-UP" case they are ~ 45° to each other. A

detailed theoretical discussion of the $\vec{s}, \vec{p}$ vectors based on the absorption or other model might use the experimentally measured $\vec{s}, \vec{p}$ vectors to resolve the phase shift ambiguity.

It has been quite fruitful analyzing the data compilation in these two ways: moment analysis and pole extrapolation. Comparison of results from the two methods appear to have clarified many of the problems in $\pi\pi$ scattering.

FOOTNOTES AND REFERENCES

*Work supported in part by the U.S. Atomic Energy Commission.

[1] P. E. Schlein, Phys. Rev. Letters 19, 1052 (1967).

[2] E. Malamud and P. E. Schlein, Phys. Rev. Letters 19, 1056 (1967).

[3] See talk by J. Haissinski, this Conference. Also S. C. C. Ting, "Electrodynamics at Small Distances, Leptonic Decays of Vector Mesons," 14th International Conference on High-Energy Physics, Vienna (1968).

[4] The following laboratories and collaborations have generously contributed their data to this analysis:

Pennsylvania-Saclay-Orasy-Bari-Bologna [V. Hagopian et al., Phys. Rev. 145, 1128 (1966), and Y. Pan, Phys. Rev. 152, 1183 (1966)].

Purdue [D. H. Miller et al., Phys. Rev. 153, 1423 (1967)].

Rochester-Yale [P. Slattery, H. Kraybill, B. Forman, and T. Ferbel, University of Rochester report UR-857-153 (1966)].

Lawrence Radiation Laboratory [S. U. Chung, Lawrence Radiation Laboratory report UCRL-16881-Rev. (1967)].

Lawrence Radiation Laboratory [D. Brown, et al., Lawrence Radiation Laboratory report UCRL-17665 (1967); D. Brown, Lawrence Radiation Laboratory report UCRL-18254 (1968)].

Lawrence Radiation Laboratory [L. Jacobs, Lawrence Radiation Laboratory report UCRL-16877, (1966)].

Lawrence Radiation Laboratory [G. Goldhaber, et al., Phys. Rev. Letters 12, 336 (1964)].

University of California, San Diego [Maris Abolins, et al., Phys. Rev. Letters 11, 381 (1963)].

Brookhaven National Laboratory [V. E. Barnes et al., Phys. Rev. Letters 16, 41 (1966)].

Argonne-Toronto-Wisconsin [D. R. Clear, et al., Nuovo Cimento 49A, 399 (1967); A. W. Key, et al., Phys. Rev. 166, 1430 (1968)].

Columbia-Rutgers [M. Rabin, R. Plano, C. Baltay, P. Franzini, L. Kirsch, H. Kung, and N. Yeh, Bull. Am. Phys. Soc. 12, 9 (1967)].

[5] J. P. Baton, G. Laurens, J. Reignier, Nuc. Phys. B3, 349 (1967); see also J. P. Baton and G. Laurens, "Determination of δ_0^2 from Chew-Low Extrapolation and Resonance t-Dependence", presented at this conference.

[6] H. P. Dürr and H. Pilkuhn, Nuovo Cimento 40, 899 (1965). See also Peter E. Schlein, "$K\pi$ Scattering and Normal Parity K^*'s", in Meson Spectroscopy, Benjamin Inc. (1968), p. 161.

[7] Z. M. Ma et al., "Pole Extrapolation Results from $pp \to \Delta^{++}n$ at 6.6 GeV/c," Phys. Rev. Letters (in press).

[8] E. Colton and Peter Schlein, "Experimental Validity of One-Pion Exchange and Prospects for Studying $\pi\pi$ and $K\pi$ Scattering," presented at this conference.

[9] E. Colton, P. E. Schlein, and E. Malamud, "Pole Extrapolation on the Reactions $\pi^- p \to \pi^-\pi^+ n$, $\pi^\pm p \to \pi^\pm\pi^-\Delta^{++}$," (to be published).

[10] G. Gidal, (private communication).

[11] M. Bander, G. L. Shaw, and J. R. Fulco, Phys. Rev. 168, 1679 (1968).

[12] Aachen et al., (German-British collaboration) Nuovo Cimento 31, 729 (1964).

[13] J. A. Poirier et al., (Notre-Dame-Pennsylvania collaboration) Phys, Rev. 163, 1462 (1967).

[14] J. Allitti et al., Nuovo Cimento 29, 515 (1963).

[15] G. Wolf, Phys. Rev Letters 19, 925 (1967). G. Goldhaber et al. first proposed this form factor in Phys. Letters 6, 62 (1963).

[16] The parameterization assumes only an equivalent angle $A_s = \sin\delta_s$. δ_s (600 MeV) and δ_s (900 MeV) are free parameters with linear interpolation in between. $|A_s|^2 = \sin^2\delta_s^o + \frac{1}{4}\sin^2\delta_s^2 + \sin\delta_s^o \sin\delta_s^2 \cos\left(\delta_s^o - \delta_s^2\right)$.

[17] R. C. Casella, Phys. Rev. Letters 21, 1128 (1967).

[18] J. G. Morton and D. Sinclair, "The $\pi\pi$ Phase Shift $\delta_2 - \delta_o$ from a New Measurement of the K_s branching ratio," see Proceedings of this Conference.

[19] B. Gobbi, D. Green, W. Hakel, R. Moffett, and J. Rosen, Phys. Rev. Letters 22, 682 (1969).

[20] Z. S. Strugalski, I. V. Chuvilo, I. A. Ivanovska, L. S. Okhrimenko, B. Niczyporuk, I. Kanarek, B. Stowinski, and A. Jabonski, quoted by G. Goldhaber in Proceedings of the XIIIth International Conference on High-Energy Physics, University of California Press, (1967), p. 108.

[21] M. Wahlig, E. Shibata, D. Gordon, D. Frisch, and I. Mannelli, Phys. Rev. 147, 941 (1966).

[22] E. Malamud, P. E. Schlein, T. G. Trippe, D. Brown, and G. Gidal, "Analysis of $\pi^-\pi^+$ Scattering in $\pi^+p \to \pi^-\pi^+\pi^+p$ Interactions," see Proceedings of this Conference.

[23] To make predictions for $\pi^-p \to \pi^-\pi^+n$ use

$$A_s^{\pi^-\pi^+} = \frac{2}{3}A_s^{o} + \frac{1}{3}A_s^{2}, \quad A_p^{\pi^-\pi^+} = A'p.$$

The amplitudes used in Ref. 2 were inadvertantly a factor of 1/2 too small, although this did not affect any of the numerical results.

Table II. Down-Up Solutions.

Fit	α (without resolution)	β (without resolution)	γ (with resolution)
Mass range (MeV)	600 - 900	400 - 1000	600 - 900
No. of parameters	30	40	30
No. of constraints	498	668	498
χ^2	521.1	753.9	533.9
Confidence level	0.229	0.012	0.129
A_1 $(\mu b/MeV\ GeV^2)^{\frac{1}{2}}$	21.9	21.9	17.5
Parameters			
b_1 (GeV^{-2})	7.09 ± 0.19	6.80 ± 0.47	7.10 ± 1.19
A_2 $(\mu b/MeV\ GeV^2)^{\frac{1}{2}}$	26.0 ± 1.6	25.3 ± 0.7	23.5 ± 0.3
b_2 (GeV^{-2})	7.33 ± 0.23	7.36 ± 0.24	7.38 ± 0.35
A_3 (radians)	0.56 ± 0.07	0.57 ± 0.07	0.53 ± 0.08
b_3 (GeV^{-2})	-0.70 ± 1.68	-2.01 ± 0.18	-0.36 ± 0.19
A_4 $(\mu b/MeV\ GeV^2)^{\frac{1}{2}}$	7.3 ± 0.4	7.0 ± 0.2	6.6 ± 0.06
b_4 (GeV^{-2})	-0.84 ± 0.31	-0.65 ± 0.14	-0.78 ± 0.40
A_5 (radians)	1.63 ± 0.25	1.65 ± 0.27	1.64 ± 0.56
b_5 (GeV^{-2})	7.75 ± 2.16	6.40 ± 2.53	8.15 ± 7.64
A_6 $(\mu b/MeV\ GeV^2)^{\frac{1}{2}}$	10.2 ± 0.6	9.7 ± 0.4	9.4 ± 0.6
b_6 (GeV^{-2})	2.03 ± 0.36	2.01 ± 0.30	2.12 ± 0.06
a (GeV^{-1})	-0.18 ± 1.26	-0.86 ± 0.24	0.09 ± 0.90
b (GeV^{-2})	4.6 ± 10.8	9.9 ± 1.1	6.6 ± 16.4
m_ρ (MeV)	775.0 ± 0.8	775.5 ± 2.1	769.0 ± 5.6
Γ_ρ (MeV)	154.7 ± 16.6	155.4 ± 5.5	155.4 ± 24.7
Phase shift at:			
420 (MeV)		13° ± 3°	
460		19 ± 3	
500		22 ± 3	
540		23 ± 3	
580		29 ± 3	
610	37° ± 10°	32 ± 3	42° ± 8°
630	50 ± 13	42 ± 4	50 ± 5
650	46 ± 10	39 ± 4	45 ± 10
670	42 ± 7	41 ± 3	48 ± 6
690	56 ± 13	53 ± 6	57 ± 8
710	72 ± 7	71 ± 6	69 ± 7
730	70 ± 10	69 ± 14	70 ± 7
750	80 ± 10	80 ± 11	78 ± 7
770	96 ± 10	96 ± 11	96 ± 6
790	106 ± 13	105 ± 11	107 ± 8
810	132 ± 6	132 ± 5	139 ± 7
830	138 ± 6	136 ± 5	142 ± 7
850	148 ± 5	148 ± 5	156 ± 6
870	146 ± 6	146 ± 5	152 ± 8
890	138 ± 9	138 ± 6	146 ± 8
910		138 ± 6	
930		154 ± 6	
950		144 ± 7	
970		160 ± 5	
990		172 ± 5	

Table III. Up-Up Solutions.

Fit	α (without resolution)	β (without resolution)	γ (with resolution)	δ (with resolution)
Mass Range (MeV)	600 - 900	400 - 1000	600 - 900	480 - 1000
No. of parameters	30	40	30	38
No. of constraints	498	668	498	652
χ^2	497.9	730.2	507.9	721.7
Confidence level	0.495	0.043	0.379	0.036
A_1 (μb/MeV GeV^2)	16.5	16.5	16.4	15.5
Parameters				
b_1 (GeV^{-2})	6.89 ± 0.51	6.63 ± 0.43	7.48 ± 0.50	7.89 ± 0.65
A_2 (μb/MeV GeV^2)$^{\frac{1}{2}}$	24.8 ± 1.5	25.7 ± 1.3	23.4 ± 1.6	22.1 ± 2.0
b_2 (GeV^{-2})	7.40 ± 0.24	7.43 ± 0.22	7.26 ± 0.22	7.19 ± 0.24
A_3 (radians)	0.01 ± 0.06	0.01 ± 0.06	0.01 ± 0.03	0.01 ± 0.18
b_3 (GeV^{-2})	10.3 ± 20.6	15.2 ± 21.0	-0.3 ± 13.6	-8.1 ± 0.1
A_4 (μb/MeV GeV^2)$^{\frac{1}{2}}$	7.6 ± 1.4	8.5 ± 1.0	7.2 ± 0.2	7.1 ± 2.2
b_4 (GeV^{-2})	-0.47 ± 1.05	0.00 ± 0.67	-0.36 ± 0.60	-0.21 ± 1.28
A_5 (radians)	1.59 ± 0.24	1.66 ± 0.19	1.6 ± 0.20	1.61 ± 0.17
b_5 (GeV^{-2})	13.8 ± 3.2	11.5 ± 2.40	13.9 ± 2.5	11.9 ± 5.6
A_6 (μb/MeV GeV^2)$^{\frac{1}{2}}$	10.1 ± 0.6	10.5 ± 0.2	9.5 ± 0.2	8.8 ± 0.7
b_6 (GeV^{-2})	1.94 ± 0.29	1.82 ± 0.16	1.96 ± 0.20	1.63 ± 0.11
a (GeV^{-1})	0.67 ± 0.59	1.06 ± 0.36	0.48 ± 0.66	0.38 ± 0.08
b (GeV^{-2})	-1.4 ± 5.6	4.66 ± 2.38	3.0 ± 7.8	4.08 ± 2.68
m_ρ (MeV)	771.9 ± 3.1	767.4 ± 1.5	772.3 ± 4.5	772.6 ± 2.8
Γ_ρ (MeV)	160.7 ± 11.5	153.7 ± 7.0	154.8 ± 13.3	158.4 ± 8.7
Phase shift at:				
420 (MeV)		25° ± 4°		
460		36 ± 5		
500		42 ± 5		41° ± 5°
540		45 ± 5		42 ± 6
580		54 ± 5		46 ± 6
610	57° ± 6°	56 ± 6	51° ± 6°	50 ± 7
630	76 ± 6	75 ± 6	67 ± 7	65 ± 7
650	70 ± 6	69 ± 6	60 ± 8	57 ± 9
670	53 ± 7	53 ± 7	49 ± 6	48 ± 6
690	80 ± 7	81 ± 7	69 ± 9	66 ± 13
710	77 ± 6	76 ± 6	67 ± 8	66 ± 8
730	95 ± 6	95 ± 7	91 ± 7	88 ± 9
750	97 ± 9	96 ± 10	95 ± 10	92 ± 11
770	93 ± 10	96 ± 11	98 ± 9	95 ± 5
790	111 ± 10	110 ± 10	117 ± 9	113 ± 11
810	133 ± 5	135 ± 5	145 ± 5	144 ± 6
830	138 ± 6	139 ± 5	148 ± 5	147 ± 6
850	149 ± 5	151 ± 5	160 ± 5	160 ± 5
870	146 ± 6	148 ± 5	159 ± 5	159 ± 5
890	138 ± 9	142 ± 6	150 ± 8	150 ± 6
910		146 ± 5		140 ± 11
930		161 ± 5		172 ± 5
950		159 ± 4		155 ± 9
970		164 ± 5		166 ± 8
990		175 ± 5		186 ± 6

Table IV. Up-Down Solutions.

Fit	α (without resolution)	β (without resolution)	γ (with resolution)
Mass Range (MeV)	600 - 900	400 - 1000	600 - 900
No. of parameters	30	40	30
No. of constraints	498	668	498
χ^2	504.7	737.2	512.6
Confidence level	0.415	0.034	0.299
A_1 $(\mu b/MeV\ GeV^2)^{\frac{1}{2}}$	16.5	16.2	15.6
Parameters			
b_1 (GeV^{-2})	6.90 ± 0.51	6.49 ± 0.45	7.09 ± 0.55
A_2 $(\mu b/MeV\ GeV^2)^{\frac{1}{2}}$	25.2 ± 1.5	27.5 ± 1.4	25.0 ± 1.7
b_2 (GeV^{-2})	7.37 ± 0.25	7.41 ± 0.23	7.29 ± 0.26
A_3 (radians)	0.013 ± 0.058	0.016 ± 0.065	0.063 ± 0.060
b_3 (GeV^{-2})	10.2 ± 17.8	8.6 ± 21.4	-6.2 ± 19.0
A_4 $(\mu b/MeV\ GeV^2)^{\frac{1}{2}}$	7.3 ± 0.8	8.1 ± 0.8	7.4 ± 1.0
b_4 (GeV^{-2})	-0.84 ± 0.60	-0.69 ± 0.57	-0.69 ± 0.83
A_5 (radians)	1.61 ± 0.26	1.74 ± 0.22	1.62 ± 0.32
b_5 (GeV^{-2})	15.9 ± 4.0	15.1 ± 3.0	14.2 ± 5.5
A_6 $(\mu b/MeV\ GeV^2)^{\frac{1}{2}}$	9.9 ± 0.4	10.5 ± 0.4	9.7 ± 0.9
b_6 (GeV^{-2})	1.71 ± 0.25	1.53 ± 0.23	1.65 ± 0.49
a (GeV^{-1})	-0.08 ± 0.43	-0.10 ± 0.29	-1.11 ± 0.75
b (GeV^{-2})	-4.8 ± 4.8	0.04 ± 1.67	2.0 ± 6.8
m_ρ (MeV)	774.0 ± 2.3	772.1 ± 1.5	776.1 ± 3.9
Γ_ρ (MeV)	158.1 ± 11.4	156.6 ± 7.0	146.7 ± 11.8
Phase shift at:			
420 (MeV)		$28^\circ \pm 5^\circ$	
460		40 ± 5	
500		45 ± 5	
540		47 ± 5	
580		55 ± 5	
610	$56^\circ \pm 6^\circ$	56 ± 6	$46^\circ \pm 7^\circ$
630	74 ± 6	75 ± 6	65 ± 7
650	69 ± 6	68 ± 6	54 ± 10
670	53 ± 7	53 ± 7	48 ± 6
690	80 ± 7	78 ± 7	68 ± 8
710	77 ± 6	75 ± 6	67 ± 7
730	96 ± 6	91 ± 7	89 ± 6
750	96 ± 7	89 ± 11	93 ± 8
770	96 ± 11	83 ± 9	100 ± 9
790	96 ± 11	83 ± 6	97 ± 5
810	71 ± 5	74 ± 6	62 ± 6
830	77 ± 6	81 ± 6	70 ± 6
850	74 ± 6	76 ± 6	65 ± 6
870	84 ± 6	87 ± 7	76 ± 6
890	99 ± 7	104 ± 10	92 ± 7
910		106 ± 9	
930		83 ± 6	
950		97 ± 6	
970		92 ± 9	
990		73 ± 7	

NAL-29
2050

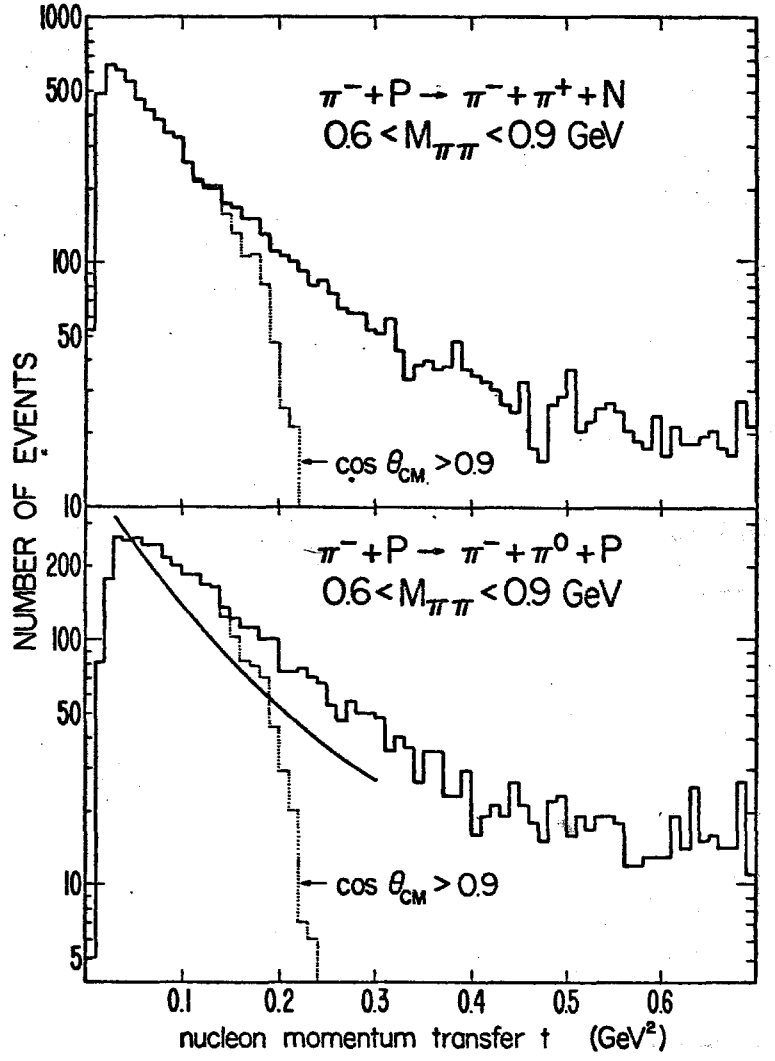

Fig. 1(a)

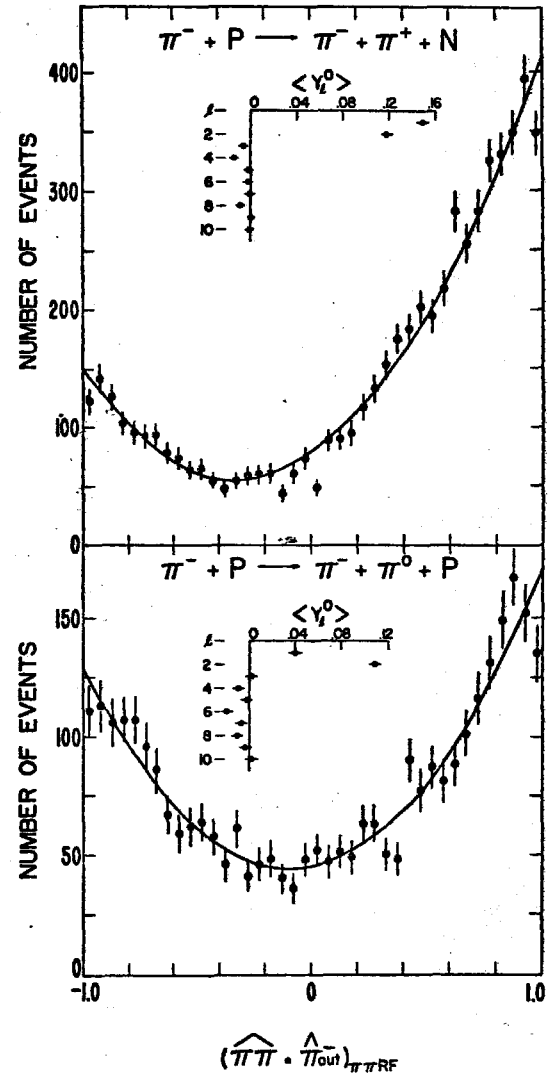

Fig. 1(b)

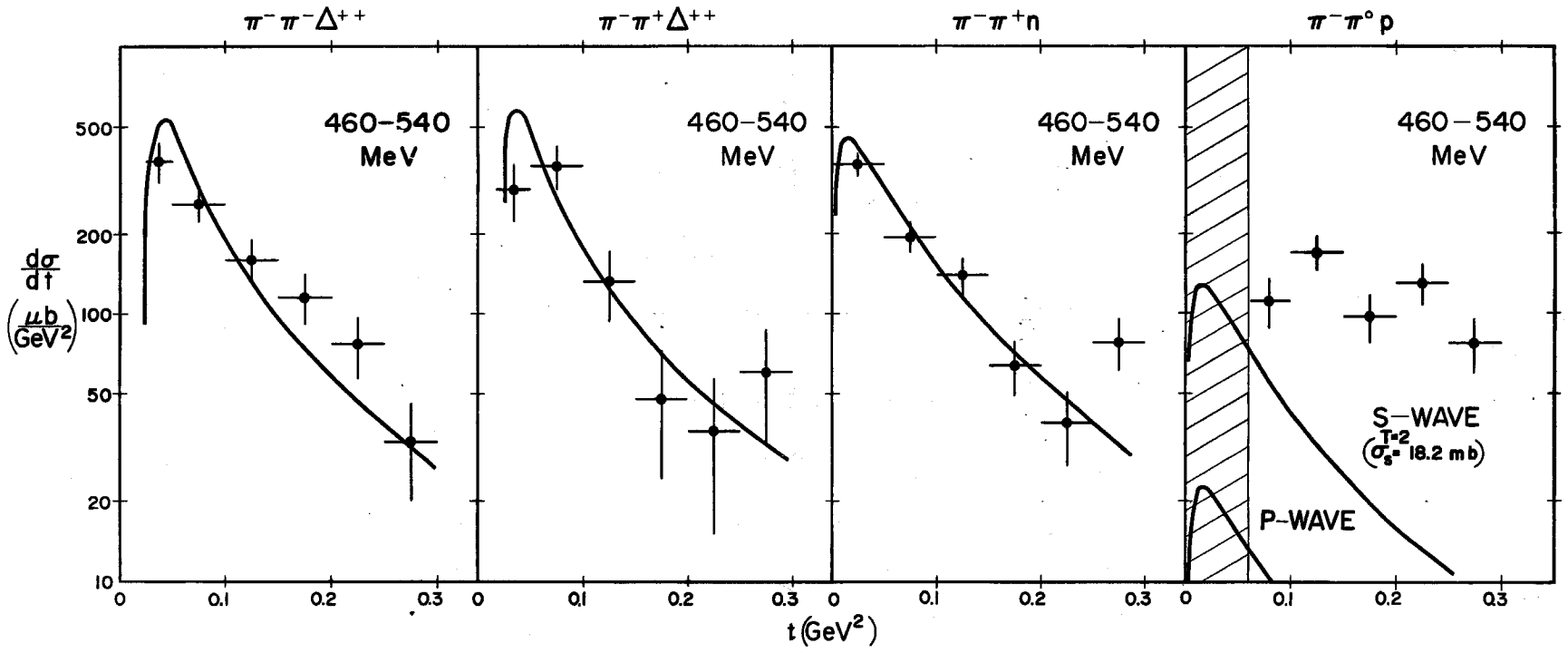
$\pi^-\pi^-\Delta^{++}$
$\pi^-\pi^+\Delta^{++}$
$\pi^-\pi^+n$
$\pi^-\pi^\circ p$
460–540 MeV
460–540 MeV
460–540 MeV
460–540 MeV
S–WAVE
$(\sigma_s^{T=2} = 18.2$ mb)
P–WAVE
$\frac{d\sigma}{dt}$ $\left(\frac{\mu b}{GeV^2}\right)$
500
200
100
50
20
10
0
0.1
0.2
0.3
t (GeV^2)

Fig. 2

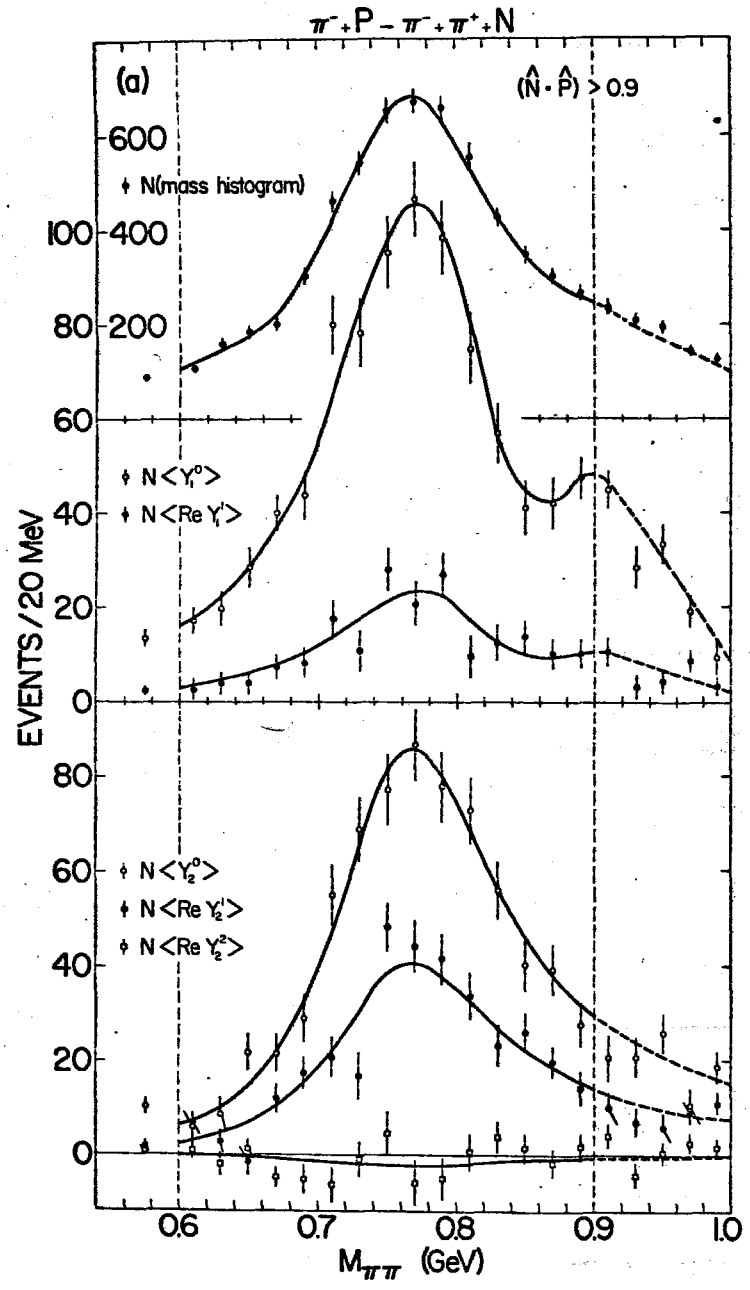
$\pi^- + P \to \pi^- + \pi^+ + N$
(a)
$(\hat{N} \cdot \hat{P}) > 0.9$
N(mass histogram)
$N\langle Y_1^0 \rangle$
$N\langle \mathrm{Re}\, Y_1^1 \rangle$
$N\langle Y_2^0 \rangle$
$N\langle \mathrm{Re}\, Y_2^1 \rangle$
$N\langle \mathrm{Re}\, Y_2^2 \rangle$
EVENTS / 20 MeV
$M_{\pi\pi}$ (GeV)

Fig. 3(a)

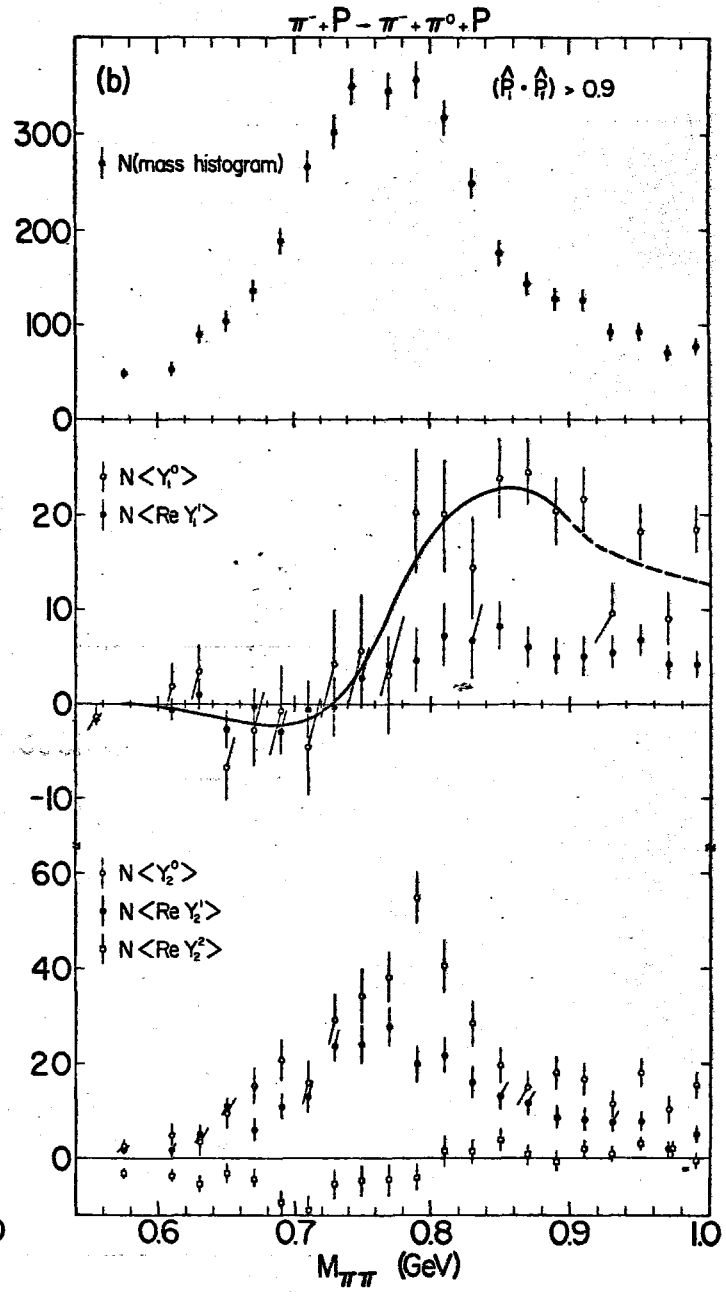
$\pi^- + P \to \pi^- + \pi^0 + P$
(b)
$(\hat{P}_f \cdot \hat{P}_i) > 0.9$
N(mass histogram)
$N\langle Y_1^0 \rangle$
$N\langle \mathrm{Re}\, Y_1^1 \rangle$
$N\langle Y_2^0 \rangle$
$N\langle \mathrm{Re}\, Y_2^1 \rangle$
$N\langle \mathrm{Re}\, Y_2^2 \rangle$
$M_{\pi\pi}$ (GeV)

Fig. 3(b)

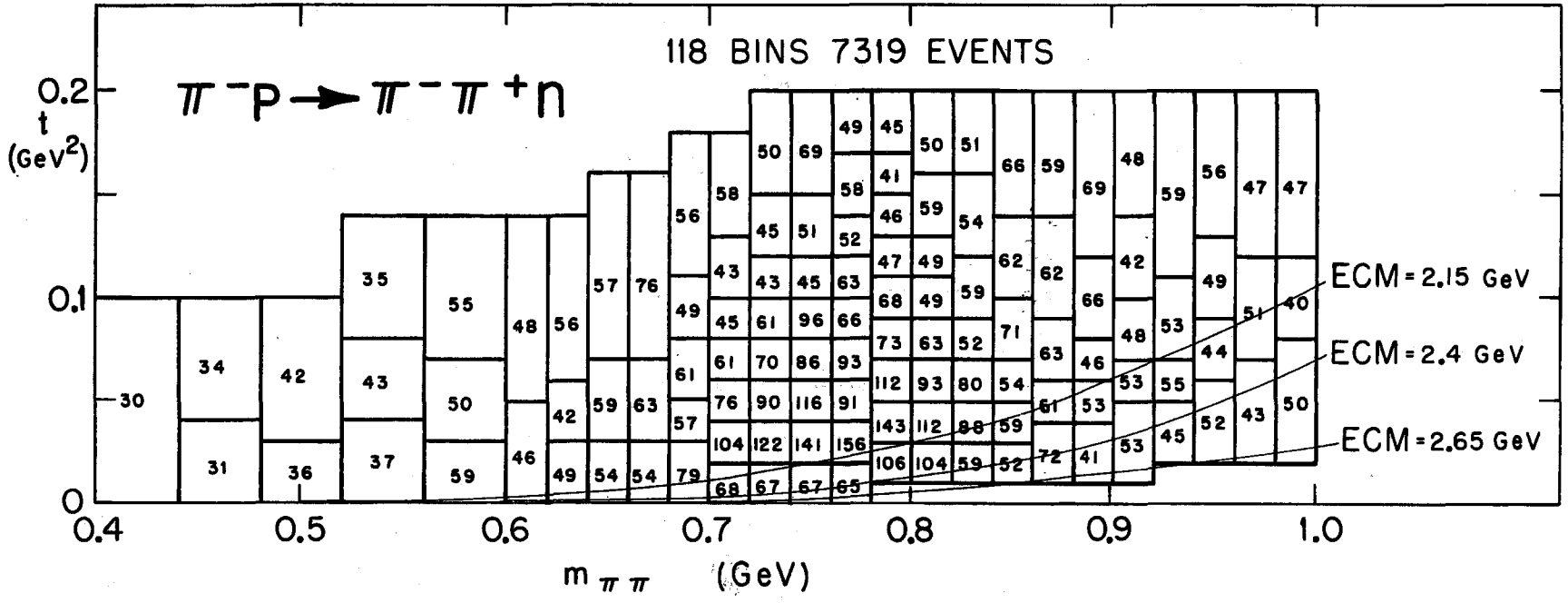
118 BINS 7319 EVENTS
$\pi^- p \rightarrow \pi^- \pi^+ n$
t (GeV^2)
0.2
0.1
0
0.4
0.5
0.6
0.7
0.8
0.9
1.0
$m_{\pi\pi}$ (GeV)
ECM = 2.15 GeV
ECM = 2.4 GeV
ECM = 2.65 GeV

Fig. 4

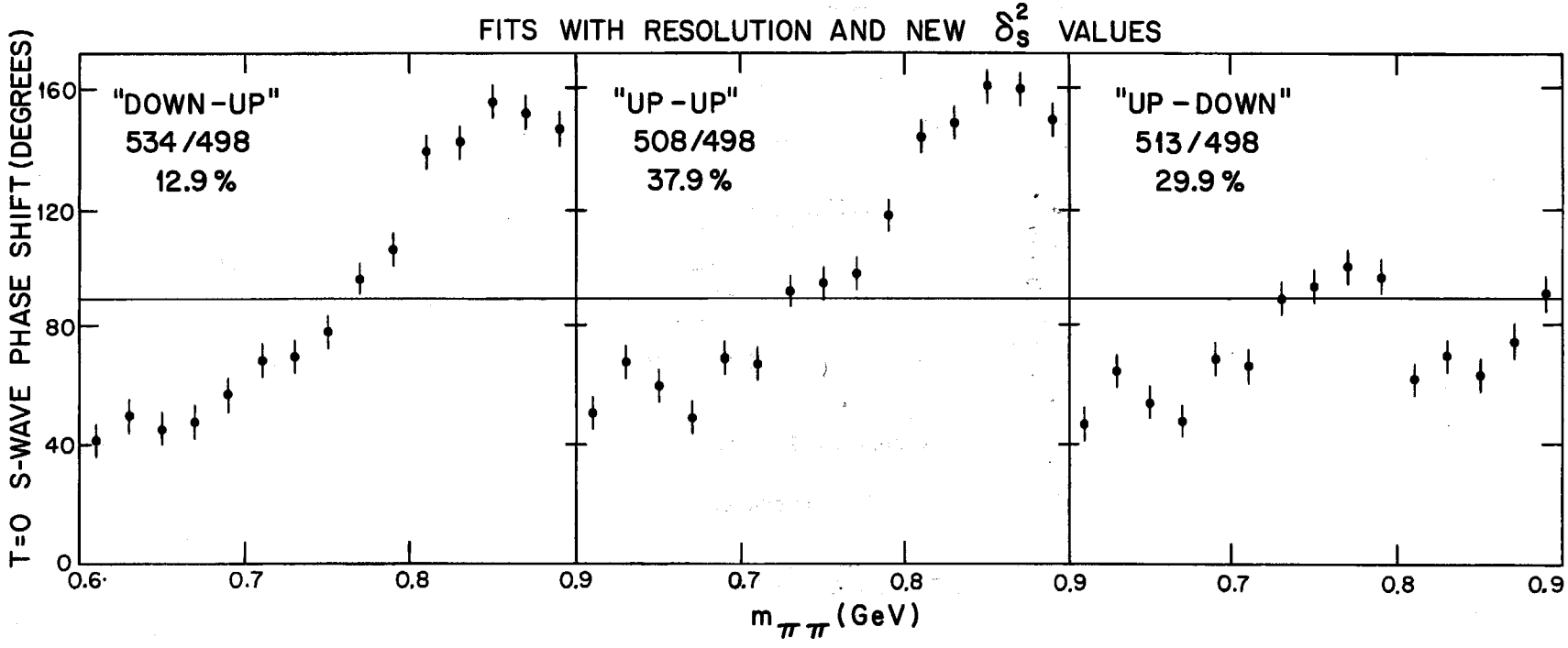

Fig. 5

NAL-29
2050

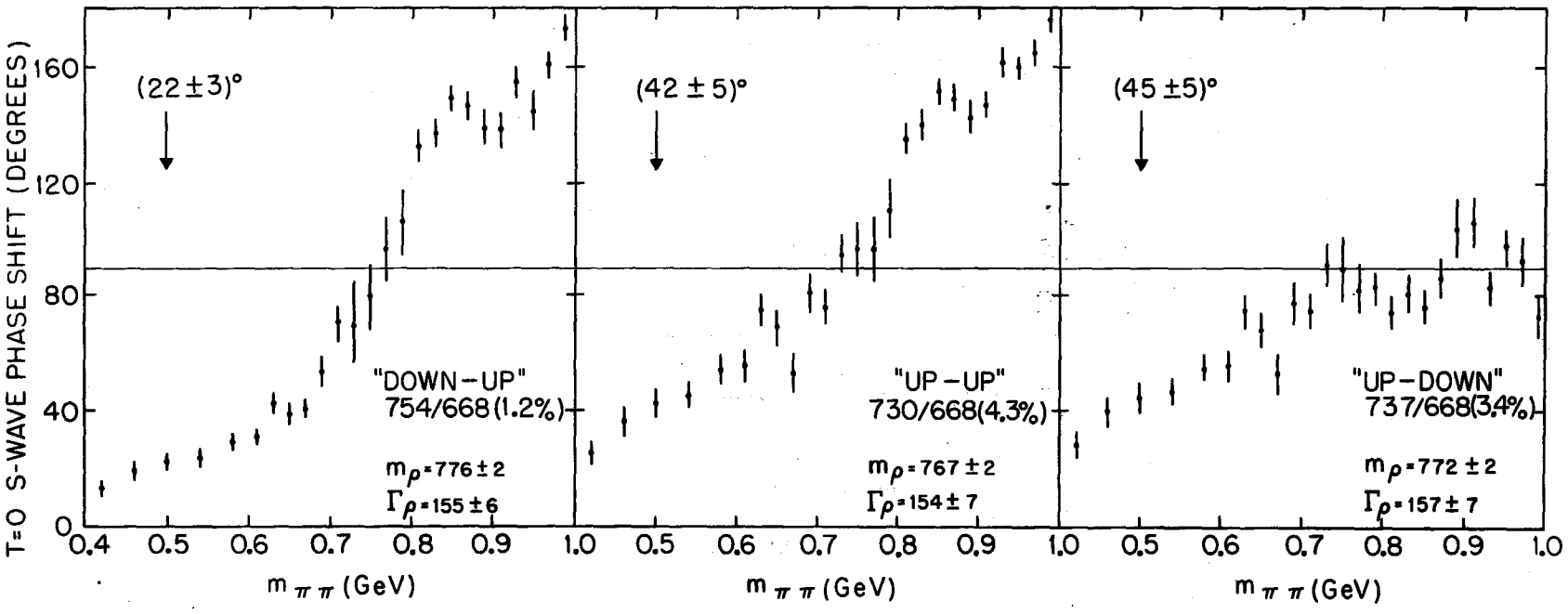
T=0 S-WAVE PHASE SHIFT (DEGREES)
160
120
80
40
0
(22 ± 3)°
(42 ± 5)°
(45 ± 5)°
"DOWN-UP"
754/668 (1.2%)
m_ρ = 776 ± 2
Γ_ρ = 155 ± 6
"UP-UP"
730/668 (4.3%)
m_ρ = 767 ± 2
Γ_ρ = 154 ± 7
"UP-DOWN"
737/668 (3.4%)
m_ρ = 772 ± 2
Γ_ρ = 157 ± 7
0.4 0.5 0.6 0.7 0.8 0.9 1.0
$m_{\pi\pi}$ (GeV)

Fig. 6

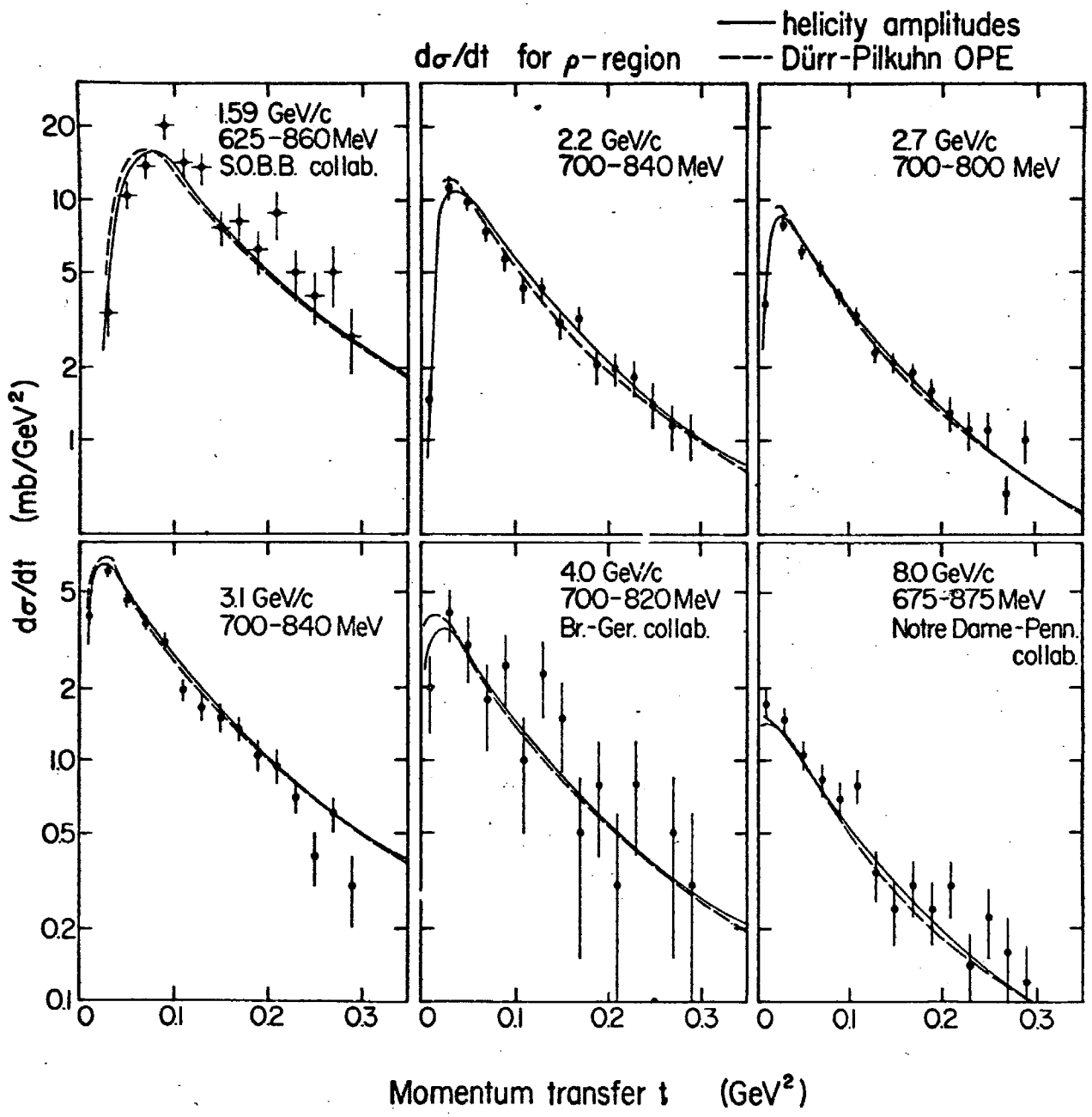
helicity amplitudes
Dürr-Pilkuhn OPE
dσ/dt for ρ-region
1.59 GeV/c
625-860 MeV
S.O.B.B. collab.
2.2 GeV/c
700-840 MeV
2.7 GeV/c
700-800 MeV
3.1 GeV/c
700-840 MeV
4.0 GeV/c
700-820 MeV
Br.-Ger. collab.
8.0 GeV/c
675-875 MeV
Notre Dame-Penn. collab.
dσ/dt (mb/GeV²)
Momentum transfer t (GeV²)

Fig. 7

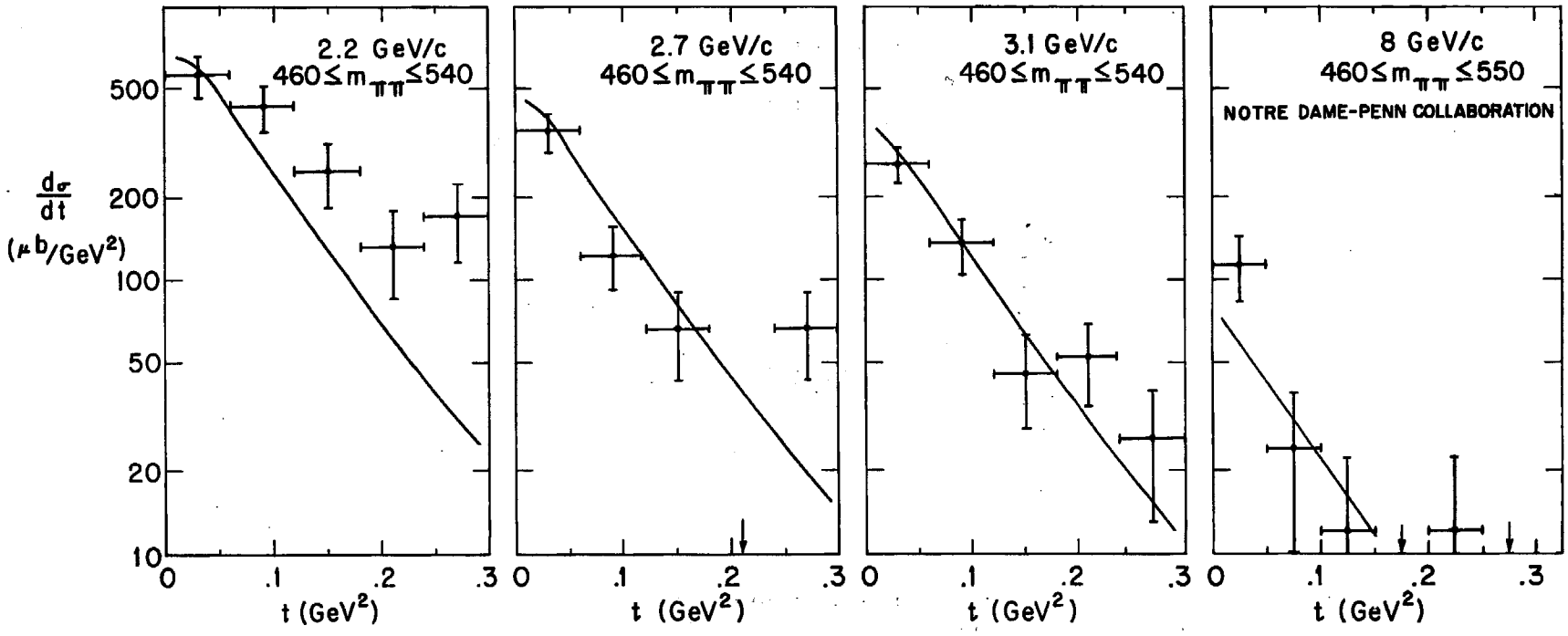
2.2 GeV/c
460≤m_ππ≤540
2.7 GeV/c
460≤m_ππ≤540
3.1 GeV/c
460≤m_ππ≤540
8 GeV/c
460≤m_ππ≤550
NOTRE DAME-PENN COLLABORATION
dσ/dt
(μb/GeV²)
500
200
100
50
20
10
0
.1
.2
.3
t (GeV²)

Fig. 8.